Dalton Transactions

RSC Publishing

PAPER

View Article Online
View Journal | View Issue

Cite this: *Dalton Trans.*, 2013, **42**, 14134

Kinetic and mechanistic investigation of the substitution reactions of four and five co-ordinated rhodium stibine complexes with a bulky phosphite†

Clare Hennion,[a] Klara J. Jonasson,[b] Ola F. Wendt*[b] and Andreas Roodt*[a]

Received 30th June 2013,
Accepted 26th July 2013

DOI: 10.1039/c3dt51757h

www.rsc.org/dalton

The substitution reaction of *trans*-[Rh(Cl)(CO)($SbPh_3$)$_2$] (**1**) with tris(2,4-di-*tert*-butylphenyl)phosphite (2,4-TBPP) to form *trans*-[Rh(Cl)(CO)(2,4-TBPP)$_2$] (**4**) in two consecutive steps has been investigated by UV-vis stopped-flow spectrophotometry. The experiments were performed in dichloromethane and in ethyl acetate, at 298 K and 268 K respectively for the first reaction step, and for the second reaction step over a temperature range from 278 to 313 K in both solvents. The first step is very fast (up to 1630 s^{-1}) and on the limit of what is observable with the stopped-flow technique. Introduction of the five-coordinate complex *trans*-[Rh(Cl)(CO)($SbPh_3$)$_3$] (**2**) in equilibrium with (**1**), by adding an excess $SbPh_3$, led to a significant decrease in overall reaction rate for the formation of the intermediate *trans*-[Rh(Cl)(CO)($SbPh_3$)$_2$(2,4-TBPP)] (**3**). Activation parameters for the second substitution reaction, in which **3** is converted to **4**, has been determined as $\Delta H^{\ddagger}$ = 22.85 ± 0.17 and 28.38 ± 0.10 kJ mol^{-1} and $\Delta S^{\ddagger}$ = −144.7 ± 0.6 and −100.9 ± 0.4 J mol^{-1} K^{-1} for CH_2Cl_2 and EtOAc respectively, supporting an associative pathway. A strongly coordinating solvent promotes both reactions. In all reaction steps a strong tendency for stibines to promote 5-coordinated, fairly stable intermediates is manifested.

Introduction

Transition metal complexes of tertiary phosphine ligands remain one of the most frequently studied areas of coordination chemistry, and examples of tertiary arsine complexes are also frequently occurring in the literature.[1] In contrast, structure and reactivity investigations of complexes with heavier pnictogen donor atoms, *i.e.* stibines and bismuthines, have received limited attention.[2,3] In part, this reflects their significantly weaker coordination ability, along with the lack of a convenient NMR probe analogous to the ^{31}P nucleus. Still, there have been reports of stibines being incorporated into modified cobalt catalyst systems for amidocarbonylation reactions, giving improved catalytic activity and yields comparable to the classic cobalt phosphine systems.[4] Moreover, there are examples of a stibine-modified Wilkinson's catalyst and [$Co_2(CO)_8$] catalysts increasing the aldehyde yield and *n* : iso ratio in the homogeneous hydroformylation of α-olefins under syngas,[5] underlining the importance of further investigations on similar systems. In both cobalt[6] and rhodium[7] catalysed hydroformylation reactions, the introduction of sterically demanding phosphite ligands has been shown to give high turn-over rates.[8] Thus, in general, little is known about the fundamental reactivity of group 9 stibine complexes and we decided to rectify this paucity of information.

Here we report on the kinetics and mechanism for the two consecutive substitution reactions of *trans*-[Rh(Cl)(CO)($SbPh_3$)$_2$] (**1**) with the bulky phosphite tris(2,4-di-*tert*-butylphenyl)phosphite (2,4-TBPP).

Experimental

General procedures and materials

The solvents used in the kinetic experiments were of analytical grade and were pre-dried by passage over alumina (neutral, Brockmann grade I) and then dried according to literature procedures prior to use.[9] Tris(2,4-di-*tert*-butylphenyl)phosphite (Aldrich, 98%) was purchased and used as previously described.[10] All other solvents and reagents were purchased and used as received. Infrared spectra were recorded as KBr disks or in $CHCl_3$ using a Bruker Equinox FT-IR spectrophotometer and analysed using the Bruker OPUS-NT software. The UV-vis spectra were recorded using a Varian Cary 50 spectrophotometer with 1.00 cm path length cells. ^{1}H and ^{31}P{^{1}H}

[a]*Department of Chemistry, University of the Free State, P.O. Box 339, Bloemfontein, 9300, South Africa. E-mail: roodta@ufs.ac.za; Fax: +27 (0)51 4446384; Tel: +27 (0)51 401 2547*
[b]*Centre for Analysis and Synthesis, Department of Chemistry, Lund University, P.O. Box 124, S-22100 Lund, Sweden. E-mail: ola.wendt@chem.lu.se*
†Electronic supplementary information (ESI) available. See DOI: 10.1039/c3dt51757h

NMR spectra were recorded using a Varian Gemini 300 MHz instrument, operating at 300 and 75 MHz for each nucleus respectively.

Synthesis and characterization

Compound **1** was prepared according to the original synthesis[2] and characterised by IR and UV-vis spectroscopy. The final compound (**4**) was characterised by IR and ^{31}P NMR spectroscopy, and the data were in agreement with those for the same complex synthesised directly from the rhodium dimer $[Rh(\mu\text{-}Cl)(CO)_2]_2$.[11]

Kinetic measurements

Stopped-flow kinetic measurements were performed using an Applied Photophysics Bio Sequential SX-17 MX stopped-flow spectrophotometer. The two consecutive substitutions of the stibine ligands in **1** by 2,4-TBPP were studied in ethyl acetate and dichloromethane, by observing the decrease of absorbance at 310 nm in both solvents. The complex solution (2.5×10^{-4} mol dm^{-3}) was mixed directly in the stopped-flow instrument with an equal volume of phosphite solution ($\geq 2.5 \times 10^{-3}$ mol dm^{-3}) ensuring pseudo first-order conditions. The variable temperature experiments were conducted between 268 and 313 K. The rate constants were obtained from least-squares fits of the absorbance *vs.* time traces to a first-order model using the software supplied by Applied Photophysics.[12] The rate constants are reported as the average of at least five kinetic runs. Some of the measured rate constants are very high but due to the short dead-time and the high change in absorbance, it was possible to follow the later part of reactions with as high rate constants as 2200 s^{-1} and evaluate the rate with a reasonable accuracy (around 5% error). The highest rate constant used was 1630 s^{-1}. A limiting and typical example is shown in Fig. S2a and b,† respectively.

Results and discussion

Stoichiometry

Fig. 1a shows the infrared spectrum of the carbonyl absorption peaks following the addition of 2,4-TBPP to **1**. The peaks shift towards higher wave number following the trend expected with the metal centre becoming less electron dense with each stibine substitution and phosphite incorporation. The spectrum displays two isosbestic points at 1982 and 2002 cm^{-1} respectively, corresponding to the two consecutive substitution reactions. The observed intermediate at 1994 cm^{-1} could not be isolated for characterisation, but we postulate it to be the five-coordinate complex **3** (Scheme 1) for reasons developed below and in the Kinetics section. The ^{31}P NMR spectra in Fig. 1b are also in agreement with the postulated reaction scheme; compounds **3** and **4** are formed consecutively and **4** is assigned as a bis-phosphinite complex based on the intensity and the lower coupling constant in agreement with the higher *trans* influence of the phosphinite compared to the stibine.

Mixing **1** and 2,4-TBPP in equimolar amounts gave compound **3** in high yield in solution. However, by allowing this mixture to equilibrate for 24 h, the formation of both **4** and **1** is observed, indicating reversibility in the overall reaction, *i.e.* in both steps.

An IR spectrum of this mixture is shown in Fig. 2. From this, approximate equilibrium constants K_1 and K_2 of

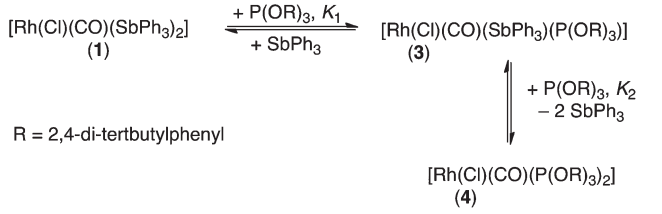

Scheme 1 General mechanism for the two consecutive substitution reactions to form (**4**) from (**1**).

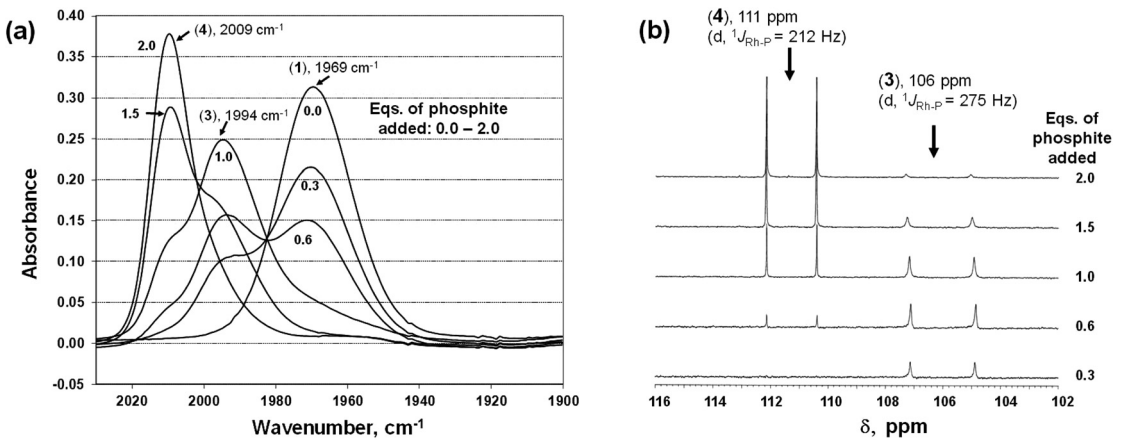

Fig. 1 (a) Changes in the IR spectra for the addition of 2,4-TBPP to *trans*-$[Rh(Cl)(CO)(SbPh_3)_2]$ (**1**) in $CHCl_3$ at T = 25 °C. [Rh] = 5 mmol dm^{-3}, [2,4-TBPP] correspond to 0, 1.5, 3, 5, 7.5 and 10 mmol dm^{-3} for 0, 0.3, 0.6, 1.0, 1.5 and 2.0 equivalents respectively. (b) ^{31}P NMR following 2,4-TBPP addition to $[Rh(Cl)(CO)(SbPh_3)_2]$ (**1**) in $CDCl_3$ at 25 °C. [Rh] = 11.5 mmol dm^{-3}, [2,4-TBPP] = 3.5, 6.9, 11.5, 17.3 and 23 mmol dm^{-3} for 0.3, 0.6, 1, 1.5 and 2.0 equivalents respectively.

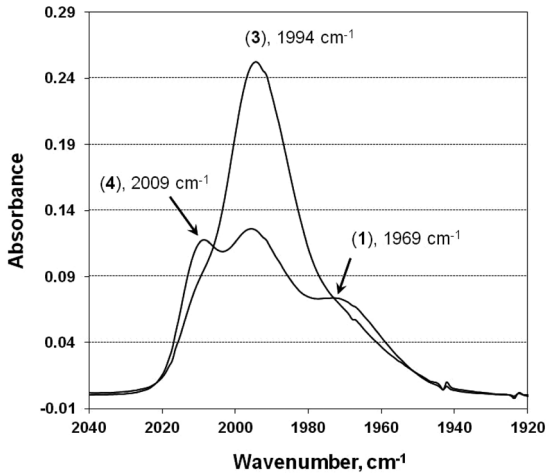

Fig. 2 Changes in the IR spectrum of compound **3** as a function of time, generated by the addition of one equivalent of 2,4-TBPP to *trans*-[Rh(Cl)(CO)-($SbPh_3$)$_2$] (**1**) in $CHCl_3$ at T = 25 °C to yield (**3**), [Rh] = 5 mmol dm^{-3}, [2,4-TBPP] = 5 mmol dm^{-3} (= 1.0 equivalent), at *ca.* 0 h and 24 h respectively.

$(3.0 \pm 0.9) \times 10^3$ mol^{-1} dm^3 and $(2.5 \pm 0.7) \times 10^{-2}$ mol dm^{-3} can be extracted (see ESI†).

Kinetics

Preliminary kinetic results show that there are two time-resolved events which we ascribe to the two reactions in Scheme 1, and Fig. S1† displays representative plots of changes in absorbance over time for the two reactions at 310 nm. The first reaction ($t_{1/2} \approx 2$ ms) is significantly faster than the second one ($t_{1/2} \approx 17$ s), allowing accurate analysis of the two reactions separately. Indeed, it was found that the first reaction step in Scheme 1 was too fast to follow under standard pseudo-first order conditions, and the observed rate constants that were calculated for higher phosphite concentrations were beyond the limits of the stopped-flow instrument.

To slow down the reaction to a manageable rate we took advantage of our previous work, which has shown that addition of an excess $SbPh_3$ to the four-coordinate complex (**1**) gives an equilibrium with the five-coordinate *trans*-[Rh(Cl)-(CO)($SbPh_3$)$_3$] (**2**).[3] Thus, the introduction of (**2**) would decrease the concentration of the bis-stibine complex (**1**), making the observation of the first step possible. Any reaction of the substantially more crowded 18-electron Rh(I) centre of (**2**) seemed highly unlikely. In addition to this modification, the reaction in ethyl acetate was carried out at −5 °C. Fig. 3 shows the observed rate constant for the first substitution step, k_{obs}^1, as a function of triphenylstibine concentration in CH_2Cl_2 and EtOAc, respectively, bearing out our assumption that the reaction is indeed strongly inhibited by the addition of excess stibine.[13] The clearly higher reactivity of the bis-stibine relative to the tris-stibine compound supports an associative attack on (**1**) for the first substitution reaction, where the crowded metal coordination sphere of the tris-stibine inhibits the attack of the entering ligand and thus gives slower substitution rates. This is also supported by the qualitative observation that the reaction is higher order in added phosphite. The data point scattering that is evident in Fig. 3b at higher concentrations refers to a limited solubility of the triphenylstibine at the low operating temperature.

Including the reversible association to a tris-stibine complex we then arrive at Scheme 2.

Assuming that (i) **2** is unreactive towards associative attack and (ii) $[Rh]_{tot} \ll [SbPh_3]$, [2,4-TBPP], the rate law for the first substitution reaction in Scheme 2 is as given in eqn (1).

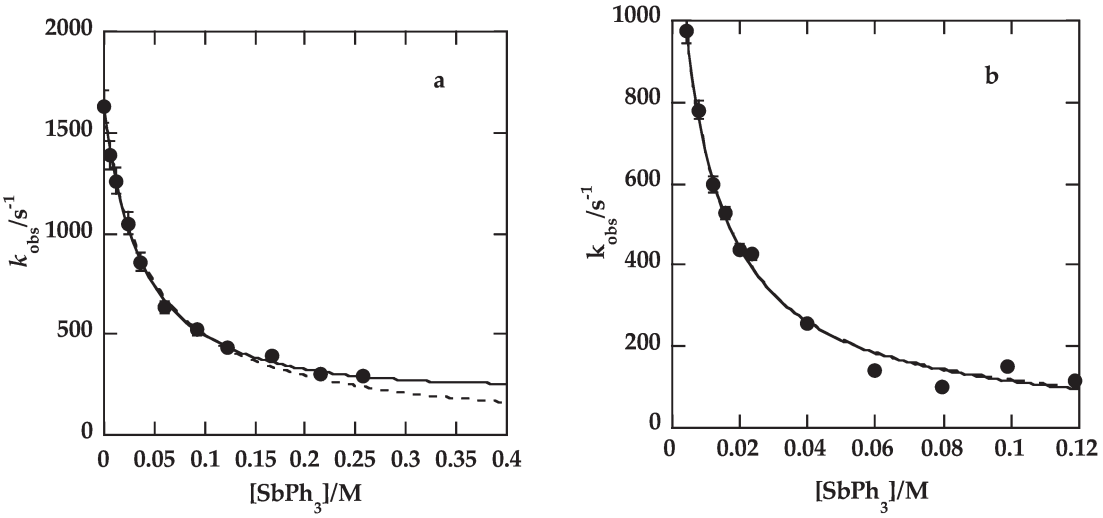

Fig. 3 Observed rate constant as a function of [$SbPh_3$] for the reaction of *trans*-[Rh(Cl)(CO)($SbPh_3$)$_2$] with 2,4-TBPP to form *trans*-[Rh(Cl)(CO)($SbPh_3$)$_2$(2,4-TBPP)] in (a) CH_2Cl_2 at T = 25 °C and (b) ethyl acetate at −5 °C. [2,4-TBPP] = 6.5 mmol dm^{-3}. The solid line denotes the best fit to eqn (1) and the dashed line the best fit to eqn (2). Error bars show errors as indicated in the ESI† (<5% (a) and <3% (b)).

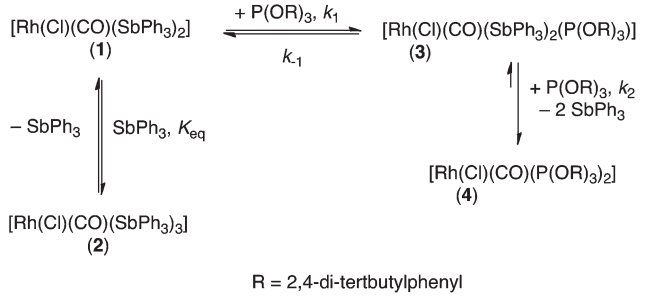

Scheme 2 Modified mechanism to form (**4**) from (**1**) and (**2**).

Table 1 Rate and equilibrium[a] constants for the formation of **3** from **1** and **2** (Scheme 2) at 25 °C and −5 °C in CH_2Cl_2 and EtOAc, respectively, using eqn (1)

(Eqn (1))	K_{eq}/mol^{-1} dm^3	$k_1/10^{-5}$ mol^{-1} dm^3 s^{-1}	$k_{-1}/10^{-2}$ s^{-1}	K_1[b]/ mol^{-1} dm^3
CH_2Cl_2 (298.2 K)	25.0 ± 1.0	6.50 ± 0.07	2.62 ± 0.06	(2.48 ± 0.06) × 10^3
EtOAc (268.2 K)	108 ± 14	5.6 ± 0.4	0 ± 2	—

[a] Assuming reversibility as predicted by Scheme 2, thermodynamic equilibrium constants for steps 1 and 2 may be estimated using IR molar absorptivities (see ESI): K_1 = [**3**]/{[**1**] [2,4-TBPP]} = (3.0 ± 0.9) × 10^3 M^{-1}, K_2 = {[**4**]·[Sb]^2}/{[**3**]·[2,4-TBPP]} = (2.5 ± 0.7) × 10^{-2} M, yielding an overall equilibrium for the complete reaction $K_o = K_1 \times K_2(7.5 \pm 3.2) \times 10$; esd's of *ca.* 30% are assumed. [b] $K_1 = k_1/k_{-1}$.

$$k_{obs}{}^1 = k_1[2,4\text{-TBPP}]/(1 + K_{eq}[SbPh_3]) + k_{-1}[SbPh_3] \quad (1)$$

Fitting the data to eqn (1) shows that it adequately describes the observed kinetics under these conditions, as illustrated in Fig. 3. The data thus obtained are reported in Table 1, also indicating good agreement between the kinetically and thermodynamically determined equilibrium constant for step 1. It can be noted that only when assuming **3** to be 5-coordinate do we arrive at good agreement between thermodynamically and kinetically determined equilibrium constants.

To test the possibility that the reversibility in the K_1-step is insignificant, we also fitted the derived rate law excluding the k_{-1}-path to the data, *cf.* Fig. 3 and eqn (2).

$$k_{obs}{}^1 = k_1[2,4\text{-TBPP}]/(1 + K_{eq}[SbPh_3]) \quad (2)$$

In ethyl acetate the fit is not significantly worse, but in dichloromethane there is a clear and systematic deviation of the fit at higher stibine concentrations. To summarise, it is thus clear that in CH_2Cl_2 the behaviour at higher stibine concentrations is not well described without assuming reversibility in the K_1-step.[14] This is of course further strengthened by the good agreement between the thermodynamically and kinetically determined equilibrium constants.

Here it can be noted that our model as outlined in Scheme 2 fits both the kinetic and equilibrium data as seen from Fig. 3 and Table 1, but if **3** is assumed to be 4-coordinate (*i.e.* if reaction 1 were a substitution rather than an association reaction) this would still be in agreement with the kinetic data (since the rate laws in eqn (1) and (2) would be the same) but there would be a large discrepancy between the IR-determined equilibrium constants and the ones obtained from the kinetics. Only when we assign compound **3** to be 5-coordinate can we explain *both* the kinetic *and* equilibrium data. At first it may seem surprising that **1** undergoes substitution *via* a spectroscopically detected 5-coordinate intermediate but one of the few documented A mechanisms was reported for a Rh stibine complex.[15]

The results of IR and ^{31}P NMR spectroscopy measurements indicate a second substitution reaction, forming **4** from **3**. Under pseudo-first-order conditions, where $[Rh]_{tot} \ll [2,4\text{-TBPP}]$, the observed rate constant is linearly dependent on phosphite concentration as indicated in eqn (3) with no observable intercept or dependence on stibine concentration ($[SbPh_3] \ll 1$). Under the kinetic conditions there is thus no observed reversibility.

$$k_{obs}{}^2 = k_2\ [2,4\text{-TBPP}] \quad (3)$$

The reaction was followed at three different temperatures over a 35 °C range and Fig. 4 shows the observed rate constant for the second substitution step $k_{obs}{}^2$ *vs.* [2,4-TBPP] in CH_2Cl_2 and EtOAc respectively. The zero intercept in Fig. 4 confirms that under the conditions employed, there is no detectable reverse reaction for the second substitution step in either solvent. This rate law is in accordance with a direct substitution as indicated in Scheme 2 (k_2-path). Fitting the second order rate constants to the Eyring equation (*cf.* Fig. S3†) gave activation parameters, and those together with the corresponding rate constants are given in Table 2. The large negative values for the entropy of activation and the low enthalpy of activation in both solvents support an associative substitution mechanism. In fact, the enthalpies are in the range typically only found for reactions involving highly π-accepting groups such as stibines and stannyl ligands, giving π-stabilisation of the transition state.[16] The fact that **3** is 5-coordinate obviously means that two stibines are lost in the reaction and the dependence on stibine concentration may be more complicated than indicated by eqn (3). Based on the current data we cannot exclude that stibine loss takes place in a fast pre-equilibrium prior to the rate determining associative attack by phosphite.

Reaction path k_1 to form *trans*-[Rh(Cl)(CO)(SbPh$_3$)$_2$(2,4-TBPP)] (**3**) is significantly faster than the following consecutive step, k_2, to form *trans*-[Rh(Cl)(CO)(2,4-TBPP)$_2$] (**4**), differing by 4–5 orders-of-magnitude. This is entirely in line with what one would expect. An associative attack on a four-coordinate complex is expected to be faster than the one on a five-coordinate complex. It is also expected that the introduction of the bulky phosphite will lower the reactivity on steric grounds.[17]

A significant difference is apparent between the two solvents from the rate constants presented in Tables 1 and 2. Even though the values of k_1 and k_{-1} were calculated at different temperatures for the two solvents and cannot be

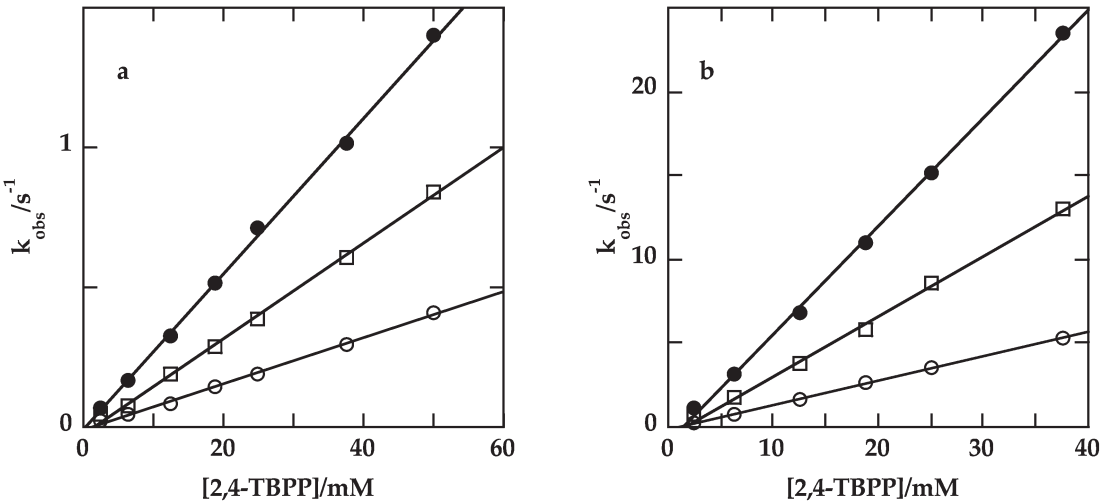

Fig. 4 Observed rate constants for the second reaction in Scheme 1 as a function of [2,4-TBPP] at different temperatures: (○) 5 °C, (□) 25 °C, and (●) 40 °C. Reaction in (a) CH_2Cl_2 and (b) ethyl acetate. [Rh] = 0.25 mmol dm^{-3}.

Table 2 Rate constants and activation parameters for the formation of **4** from **3** at 25 °C

	$k_2/M^{-1}\ s^{-1}$ (298.2 K)	$\Delta H^{\ddagger}$/kJ mol^{-1}	$\Delta S^{\ddagger}$/J K^{-1} mol^{-1}
CH_2Cl_2	17.0 ± 0.4	22.85 ± 0.17	−144.7 ± 0.6
EtOAc	355 ± 10	28.38 ± 0.10	−100.9 ± 0.4

directly compared, an increase of at least an order-of-magnitude can be expected in ethyl acetate. However, the reaction rates for the k_2 pathway allow direct comparison and display rate constants calculated for ethyl acetate exceeding those for CH_2Cl_2 by between one and two orders-of-magnitude. The equilibrium between **1** and **2** has been previously investigated by Otto and Roodt, showing that the formation of **2** is favoured in ethyl acetate over CH_2Cl_2.[2] This trend is in agreement with the obtained results for the calculated K_{eq} values: 25.0 ± 1.0 M^{-1} and 108 ± 14 M^{-1} for CH_2Cl_2 and ethyl acetate respectively, although approximately 8–12 times smaller than those determined from UV-vis thermodynamic studies. The exact reason for this observed difference is not clear from the current data. Nevertheless, the relative difference is very clear. The two solvents have similar polarities, whilst ethyl acetate has a significantly larger coordinating ability.[18] It is interesting that the higher reactivity observed in EtOAc is entirely entropic in origin, possibly due to a superior solvation of the nucleophile in the ground state. Thus, the enhanced reaction rates in ethyl acetate are supposedly attributed to the coordinating ability of the solvent. A possible explanation for this might be that the solvent coordination to the metal centre gives a Rh–Sb bond lengthening, thus opening up a larger cavity around the metal for the entering phosphite ligand. This concept would also apply to the equilibrium between **1** and **2**, where a strongly coordinating solvent enhances the formation of the five-coordinated tris-stibine **2**.

Conclusion

This study reports on the kinetics and mechanism of the two consecutive substitution reactions of a bulky phosphite ligand to the bis-stibine complex *trans*-[Rh(Cl)(CO)($SbPh_3$)$_2$]. Addition of an excess stibine significantly slowed down the reaction rate of the first step, due to the formation of a five-coordinate tris-stibine complex. Associative mechanisms have been inferred for both the first and the second substitution. A coordinating solvent has been observed to increase the reaction rate for both reaction steps. Overall, stibines strongly promote 5-coordination both in transition states and in more long-lived intermediates.

Acknowledgements

Financial support from the Swedish Research Council, the Crafoord Foundation and the Royal Physiographic Society in Lund, the South African National Research Foundation and THRIP, SIDA, the University of the Free State Strategic Academic Cluster Initiative (Materials and Nanosciences) and c*change, the DST centre of excellence in Catalysis, and SASOL is gratefully acknowledged.

References

1 (*a*) N. R. Champness, C. S. Frampton, W. Levason and S. R. Preece, *Inorg. Chim. Acta*, 1995, **233**, 43; (*b*) W. Levason, S. R. Preece and C. S. Frampton, *Polyhedron*, 1996, **15**, 2719; (*c*) P. P. Phadnis, V. J. Jain, A. Knödler and W. Kaim, *Z. Anorg. Allg. Chem.*, 2002, **628**, 1332; (*d*) L. A. van der Veen, P. K. Keeven, P. C. J. Kamer and P. W. N. M. van Leeuwen, *Chem. Commun.*, 2000, 333; (*e*) V. K. Srivastava, S. K. Sharma, R. S. Shukla,

N. Subrahmanyam and R. V. Jasra, *Ind. Eng. Chem. Res.*, 2005, **44**, 1764.

2 (*a*) N. R. Champness and W. Levason, *Coord. Chem. Rev.*, 1994, **133**, 115; (*b*) O. F. Wendt and L. I. Elding, *J. Chem. Soc., Dalton Trans.*, 1997, 4725; (*c*) W. Levason and G. Reid, *Coord. Chem. Rev.*, 2006, **250**, 2565; (*d*) S. Otto and S. N. Mzamane and A. Roodt, in *Modern Coordination Chemistry: Legacy of Joseph Chatt*, ed. N. Winterton and G. Leigh, Royal Society of Chemistry, Cambridge, UK, 2001, p. 675; (*e*) S. Otto and A. Roodt, *Acta Crystallogr., Sect. C: Cryst. Struct. Commun.*, 2002, **58**, 565; (*f*) S. Otto and A. Roodt, *Inorg. Chim. Acta*, 2004, **357**, 1; (*g*) S. Otto and A. Roodt, *Inorg. Chem. Commun.*, 2004, **11**, 114.

3 S. Otto and A. Roodt, *Inorg. Chim. Acta*, 2002, **331**, 199.

4 (*a*) R. M. Gomez, P. Sharma, L. J. Arias, J. Perez-Flores, L. Velasco and A. Cabrera, *J. Mol. Catal. A: Chem.*, 2001, **170**, 271; (*b*) A. Cabrera, P. Sharma, L. J. Arias, L. Velasco, J. Perez-Flores and R. M. Gomez, *J. Mol. Catal. A: Chem.*, 2004, **212**, 19.

5 (*a*) P. Sharma, A. Cabrera, J. L. Arias, R. Le Lagadec, R. L. Manzo and M. Sharma, *Main Group Met. Chem.*, 1995, **22**, 95; (*b*) P. Sharma, J. L. Arias, J. Vasquez, V. Gomez and R. Guiterrez, *J. Chin. Chem. Soc.*, 2007, **54**, 681.

6 (*a*) M. Haumann, R. Meijboom, J. R. Moss and A. Roodt, *Dalton Trans.*, 2004, 1679; (*b*) R. Meijboom, M. Haumann, A. Roodt and L. Damoense, *Helv. Chim. Acta*, 2005, **88**, 676.

7 (*a*) I. Odinets, T. Kégl, E. Sharova, O. Artyushin, E. Goryunov, G. Molchanova, K. Lyssenko, T. Mastryukova, G. Röschenthaler, G. Keglevich and L. Kollár, *J. Organomet. Chem.*, 2005, **690**, 3456; (*b*) O. Artyushin, I. Odinets, E. Goryunov, I. Fedyanin, K. Lyssenko, T. Mastryukova, G. Röschenthaler, T. Kégl, G. Keglevich and L. Kollár, *J. Organomet. Chem.*, 2006, **691**, 5547.

8 P. W. N. M. van Leeuwen and C. F. Roobeek, *J. Organomet. Chem.*, 1983, **258**, 343.

9 D. D. Perrin and W. L. F. Armarego, *Purification of Laboratory Chemicals*, Pergamon Press, Oxford, UK, 3rd edn, 1988.

10 R. Crous, M. Datt, D. Foster, L. Bennie, C. Steenkamp, J. Huyser, L. Kirsten, G. Steyl and A. Roodt, *Dalton Trans.*, 2005, 1108.

11 L. Kirsten, MSc dissertation, University of Johannesburg, South Africa, 2005.

12 Bio Sequential SX-17MV Stopped-flow ASVD Spectrophotometer, software manual, Applied Photophysics Ltd., 1994, 203/205 Kingston Road, Leatherhead, UK KT22 7PB.

13 In principle, a dissociative mechanism would also explain the inhibition observed, but from ref. 3 we know that complex 1 undergoes association and furthermore a dissociative mechanism does not explain the behaviour at higher stibine concentrations. See Fig. S4† for more details.

14 In principle the kinetic behaviour could be explained by a parallel contribution from **1** and **2** in two concurrent processes. However, this would require a substantial contribution from the direct, associative reaction of the 18-electron species **2**. Associative reactivity of 18-electron species is unusual but there is some precedence in *e.g.* the well-known group 6 hexacarbonyls. (See M. L. Tobe and J. Burgess *Inorganic Reaction Mechanisms*; Longman Inc., New York, 1999.) In these cases the associative contribution rarely amounts to more than 10%, whereas in dichloromethane at the highest stibine concentrations it would in fact be very important in the present case, contributing some 40% at 0.25 M [$SbPh_3$]. In light of this and the fact that the kinetics is adequately described by the reversibility in the K_1-path we discarded the parallel process as an option.

15 L. Cattalini, R. Ugo and A. Orio, *J. Am. Chem. Soc.*, 1968, **90**, 4800.

16 (*a*) A. Fischer and O. F. Wendt, *J. Chem. Soc., Dalton Trans.*, 2001, 1266; (*b*) N. Kuznik and O. F. Wendt, *J. Chem. Soc., Dalton Trans.*, 2002, 3074.

17 M. R. Plutino, S. Otto, A. Roodt and L. I. Elding, *Inorg. Chem.*, 1999, **38**, 1233.

18 A. Roodt, S. Otto and G. Steyl, *Coord. Chem. Rev.*, 2003, **245**, 121.